Title

An Extended Structure—Activity Relationship of Nondioxin-Like PCBs Evaluates and Supports Modeling Predictions and Identifies Picomolar Potency of PCB 202 Towards Ryanodine Receptors

Journal

Toxicological Sciences, 155(1)

ISSN

1096-6080

Authors

Holland, Erika B

Feng, Wei

Zheng, Jing

et al.

Publication Date

2017

DOI

10.1093/toxsci/kfw189

Peer reviewed

OXFORD

SOT | Society of Toxicology
www.toxsci.oxfordjournals.org

TOXICOLOGICAL SCIENCES, 155(1), 2017, 170–181

doi: 10.1093/toxsci/kfw189
Advance Access Publication Date: September 21, 2016
Research article

An Extended Structure–Activity Relationship of Nondioxin-Like PCBs Evaluates and Supports Modeling Predictions and Identifies Picomolar Potency of PCB 202 Towards Ryanodine Receptors

Erika B. Holland,[*,†,1] Wei Feng,[*] Jing Zheng,[*,‡] Yao Dong,[*] Xueshu Li,[§] Hans-Joachim Lehmler,[§] and Isaac N. Pessah[*,¶,‖]

[*]Department of Molecular Biosciences, School of Veterinary Medicine, University of California, Davis, California; [†]Department of Biological Sciences, California State University of Long Beach, Long Beach, California; [‡]Jiangsu Provincial Key Laboratory for TCM Evaluation and Translational Development, China Pharmaceutical University, Nanjing 211198, China; [§]Department of Occupational and Environmental Health, College of Public Health, University of Iowa, Iowa City, Iowa; [¶]The Medical Investigations of Neurodevelopmental Disorders (MIND) Institute, University of California Davis Medical Center, Sacramento, California; and [‖]UC Davis Center for Children's Environmental Health and Disease Prevention, Davis, California

[1]To whom correspondence should be addressed at California State University of Long Beach, 1250 Bellflower Blvd, Long Beach, CA 90840. E-mail: erika.holland@csulb.edu.

ABSTRACT

Nondioxin-like polychlorinated biphenyls (NDL PCBs) activate ryanodine-sensitive Ca^{2+} channels (RyRs) and this activation has been associated with neurotoxicity in exposed animals. RyR-active congeners follow a distinct structure–activity relationship and a quantitative structure–activity relationship (QSAR) predicts that a large number of PCBs likely activate the receptor, which requires validation. Additionally, previous structural based conclusions have been established using receptor ligand binding assays but the impact of varying PCB structures on ion channel gating behavior is not understood. We used [^{3}H]Ryanodine ([^{3}H]Ry) binding to assess the RyR-activity of 14 previously untested PCB congeners evaluating the predictability of the QSAR. Congeners determined to display widely varying potency were then assayed with single channel voltage clamp analysis to assess direct influences on channel gating kinetics. The RyR-activity of individual PCBs assessed in *in vitro* assays followed the general pattern predicted by the QSAR but binding and lipid bilayer experiments demonstrated higher potency than predicted. Of the 49 congeners tested to date, tetra-*ortho* PCB 202 was found to be the most potent RyR-active congener increasing channel open probability at 200 pM. Shifting *meta*-substitutions to the *para*-position resulted in a $>$ 100-fold reduction in potency as seen with PCB 197. Non-*ortho* PCB 11 was found to lack activity at the receptor supporting a minimum mono-*ortho* substitution for PCB RyR activity. These findings expand and support previous SAR assessments; where out of the 49 congeners tested to date 42 activate the receptor demonstrating that the RyR is a sensitive and common target of PCBs.

Key words: nondioxin-like PCBs; ryanodine receptor; single-channel gating; neurotoxicity.

Polychlorinated biphenyls (PCBs) represent one of the leading groups of chemicals detected in environmental media and human samples (Domingo and Bocio, 2007; Faroon and Ruiz, 2015; Stahl *et al.*, 2009). Of the 209 PCB congeners, varying by the position and number of chlorine substitutions, the nondioxin-like PCBs (NDL PCB) have been identified as potential neurological toxicants due to observed cognitive deficits in PCB exposed organisms (Boix *et al.*, 2011; Lilienthal *et al.*, 2015; Schantz *et al.*, 1997, 2001; Yang *et al.*, 2009). Numerous modes of action have been described that may contribute to neurotoxicity. This includes altered neurotransmitter signaling (Fonnum and Mariussen, 2009; Mariussen and Fonnum, 2001; Wigestrand *et al.*, 2013), altered $GABA_A$ receptor activity (Fernandes *et al.*, 2010), altered Ca^{2+} homeostasis through several mechanisms (Choi *et al.*, 2016; Gafni *et al.*, 2004; Kodavanti and Tilson, 1997; Pessah *et al.*, 2010; Westerink, 2014), induced reactive oxygen species (Stenberg *et al.*, 2011), altered cell viability (Dickerson *et al.*, 2009), and alterations of neuro/endocrine processes (Bell, 2014; Fonnum and Mariussen, 2009; Kodavanti and Curras-Collazo, 2010).

Of the modes identified, a particularly sensitive endpoint is the ability of NDL PCBs to enhance the activity of ryanodine sensitive Ca^{2+} channels embedded in the sarco/endoplasmic reticulum (SR/ER), namely, the ryanodine receptor (RyR), in both mammals (Pessah *et al.*, 2006) and fish (Fritsch and Pessah, 2013). There are 3 RyR-isoforms (Berridge, 2012) with varying expression by developmental stage and brain region and the channels are essential to both peripheral and central nervous systems (for a comprehensive review see Pessah *et al.*, 2010). Briefly, RyR-isoform 1 (RyR1) and RyR-isoform 2 (RyR2) are both found to predominate in the brain, where the third isoform, RyR3, represents only about 2%. RyR Ca^{2+} release from intercellular stores contributes to neurotransmission and vesicle mobilization and cellular transcription, translation and secretion processes that are directly tied to synaptic plasticity. The RyR has also been implicated as a primary mechanism by which dendritic growth is attenuated; a measure of neuronal connectivity. In primary neuronal cultures, NDL PCB exposure increases intracellular Ca^{2+} levels, increases spontaneous Ca^{2+} oscillations (Wayman *et al.*, 2012a,b) and interferes with normal neuronal dendritic growth and plasticity in a RyR dependent manner. The expression, role and toxicity data support the RyR as a contributor to NDL PCB induced neurotoxicity and suggest that RyR-activation by NDL PCBs could disrupt several aspects of neuronal signaling.

For RyR-active PCB congeners a distinct structure–activity relationship (SAR) has been suggested (Pessah *et al.*, 2006) and the SAR is consistent for NDL PCB activity at RyR1 and RyR2 channels (Pessah *et al.*, 2010; Wong *et al.*, 1997). Congeners with 2 or more *ortho*-substitutions display high potency at the RyR whereas those lacking *ortho* substitution lack receptor activity. The most detailed SAR conducted to date has been done with RyR1, assessing RyR-activity for a subset of PCBs (35 of the 209 congeners). The SAR suggests that those congeners containing *ortho* substitution would likely contribute to neurotoxic outcomes and this prediction is supported by a recent quantitative structure–activity relationship (QSAR), which predicted the RyR activity of all 209 PCBs. The QSAR was built using the RyR1 data from previous studies (Pessah *et al.*, 2010) and predicted that approximately 190 PCBs would display RyR-activity (Rayne and Forest, 2010). Further evaluating the predictions of the *in silico* QSAR would help describe the extent to which individual congeners may contribute to mixture induced neurotoxicity.

Whereas studies have evaluated the SAR of congeners towards causing RyR activation the consequent changes in the Ca^{2+} channel's gating behavior is poorly understood. In single channel voltage clamp analysis PCB 95, thought to be the most potent RyR-active PCB, causes the RyR1 to display an increased open probability due to prolonged time in the open state together with short lived closed state transitions (Samsó *et al.*, 2009). Only 2 potent RyR active PCBs, namely, PCB 95 and enantiomers of PCB 136 (Pessah *et al.*, 2009), have been tested in single channel gating and it is unclear whether less potent RyR-active PCBs may display similar or distinct impacts on channel behavior. Studies addressing this knowledge gap would provide valuable information regarding functional changes in the RyR in the presence of various PCB congeners, especially in light of structural differences. Single channel gating is also the most direct approach for measuring the inherent potency and efficacy of compounds and mutations that modify the RyR channel (Pessah *et al.*, 2010) and could be monitored at lower concentrations.

The goals of the current study were to (1) evaluate the predictions of the previously developed QSAR by testing whether previously untested PCB congeners could alter RyR activity measured in [^{3}H]ryanodine ([^{3}H]Ry) binding assays and to (2) compare toxicity observed in [^{3}H]Ry-binding assays with changes in the RyR's functional behavior as measured through single channel voltage clamp analysis. We selected 14 congeners with 2–9 chlorine substitutions (Table 1A) that have not been previously assessed for RyR activity. Congeners were chosen based on their chlorine substitution patterns and predicted, or lack of, RyR activity (Rayne and Forest, 2010). Special focus was placed on *tetra*-ortho PCB 202, lacking *para*-substitution, which the QSAR suggested would be the most potent RyR-active congener. Additional focus was placed on PCB 11 and PCB 197, which were lacking or limited in original Aroclor mixtures (Frame, 2001; Koh *et al.*, 2015) but are detected in human serum (Koh *et al.*, 2015). As a non-*ortho* congener, PCB 11 is predicted to lack RyR-activity. PCB-197, like PCB 202, has 8 chlorines, but is predicted to have relatively lower RyR-activity due to its *para*-chloro substitutions. All the congeners selected have been detected in human samples (Koh *et al.*, 2015; Marek *et al.*, 2013; http://www.ewg.org/sites/humantoxome/chemicals/index), with several congeners, including, PCB 11, 20, 28, 95, 99, and 118, being frequently detected in both humans and the environment (Grimm *et al.*, 2015; Stahl *et al.*, 2009).

MATERIALS AND METHODS

Chemicals. Polychlorinated biphenyls (PCB) congeners were purchased neat from AccuStandard (99–100% pure). The 14 PCB congeners previously untested for RyR activity can be found in Table 1A and are displayed in comparison to 3 PCB congeners (PCB 18, 95, and 183), with published RyR-activity (Table 1B; Pessah *et al.* 2006), that were re-evaluated to provide a measure of assay reproducibility and a comparison of the current findings to that from previously published work. A stock of PCB 11 was custom synthesized (Supplementary Figs. 1 and 2) and characterized as described in the Supplementary Data. According to gas chromatography-mass spectrometric analysis and relative peak area the PCB 11 preparation was 99.99% pure (Supplementary Figs. 3 and 4).

Membrane preparation. Microsomal fractions enriched with RyR1 were created from white skeletal muscle of male New Zealand White rabbits (Pel-Freez Biologicals) as previously described (Pessah *et al.*, 1985, 1987). Briefly, muscle was ground and homogenized in buffer containing 300 mM sucrose, 10 mM 4-(2-hydroxyethyl)-1-piperazineethane sulfonic acid (HEPES), 1 pheylmethylsulfonyl fluoride and 5 μg/ml leupeptin (pH 7.4).

TABLE 1. Potency and Efficacy of PCB Congeners Toward the Ryanodine Receptor, Isoform 1, in Skeletal Muscle

A. Ryanodine receptor activity of previously untested congeners

PCB Congener	Substitution	Maximum Response (%)	EC50 (μM)	EC50 95%CI (μM)	EC_{2X} (μM)	EC_{2X} 95% CI (μM)	**Predicted EC_{2X} (μM)[b]**
11	3,3'	–	–	–	–	–	10.00
20	2,3,3'	570 ± 41	1.08	0.58–2.1	0.25	0.13–0.43	2.00
28	2,4,4'	219 ± 12	0.86	0.40–1.85	1.37	0.7– 50.00	5.00
40	2,2',3,3'	502 ± 19	1.83	1.43–2.35	0.75	0.62–0.90	1.00
44	2,2',3,5'	1374 ± 142	1.78	1.21–2.61	0.15	0.07–0.27	0.80
56	2,3,3',4'	178 ± 4	0.87	0.62–1.22	–	–	3.00
77	3,3',4,4'	134 ± 9	3.07	0.6–15.0	–	–	5.00
99	2,2',4,4',5	426 ± 25	0.74	0.44–1.23	0.28	0.20–0.37	2.00
118	2,3',4,4',5	203 ± 5	0.82	0.62–1.08	2.35	1.21–50.00	3.00
179	2,2',3,3',5,6,6'	442 ± 14	1.45	1.17–1.80	0.77	0.66–0.89	0.17
194	2,2',3,3',4,4',5,5'	618 ± 46	0.47	0.24–0.93	0.07	0.04–0.13	0.80
197[a]	2,2',3,3',4,4',6,6'	261 ± 6	1.38	1.14–1.68	1.76	1.51–2.10	0.60
202	2,2',3,3',5,5',6,6'	457 ± 45	0.31	0.08–1.10	0.05	0.02–0.10	0.12
208	2,2'3,3',4,5,5',6,6'	243 ± 21	0.03	0.003–0.11	0.10	0.03–0.42	0.18

B. Re-evaluation of previously confirmed ryanodine receptor active congeners

PCB Congener	Substitution	Maximum Response (%)	EC50 (μM)	EC50 95% CI (μM)	EC_{2X} (μM)	EC_{2X} 95% CI (μM)	Previous EC_{2X} (μM)[c]
18	2,2',5	610 ± 50	2.46	1.44–4.18	0.66	0.46–0.89	1.05
95[a]	2,2',3,5',6	1130 ± 30	0.46	0.39–0.55	0.14	0.07–0.21	0.22
183[a]	2,2',3,4,4',5',6	445 ± 21	0.82	0.51–1.32	0.35	0.16–0.61	0.55

[a]Congener displays chirality (Lehmler et al., 2010).
[b]Estimated EC_{2X} as predicted by a recent QSAR (Rayne and Forest, 2010).
[c]Previously published EC_{2X} (Pessah et al., 2006).
CI—confidence interval.

The junctional sarcoplasmic reticulum (JSR) fraction was then isolated using differential centrifugation followed by purification through a discontinuous sucrose gradient. The JSR preparation was resuspended in 300 mM sucrose and 10 mM HEPES, pH 7.4 and protein concentrations were determined in triplicate using a BCA assay (Fisher).

[^{3}H]Ryanodine binding assays. The ligand ryanodine binds preferentially to the open state of the RyR, where increased ligand binding signifies increased open state, or active state, of the receptor. We used [^{3}H]Ryanodine ([^{3}H]Ry; 61.8 Ci mmol^{-1}; Perkin Elmer) to assess the open state of the RyR in the presence of PCB congeners. Assays followed the exact experimental conditions utilized previously (Pessah *et al.*, 2006). Specifically, assays utilized 12 μg protein and 1 nM [^{3}H]Ryanodine in the presence of 0.5% DMSO or 0.01–50 μM PCB in 0.5% DMSO. Assays were conducted in 500 μL of buffer containing 140 mM KCl, 15 mM NaCl, 20 mM HEPES, and 50 μM $CaCl_2$ (pH 7.4) and incubated for 3 h at 37°C. Nonspecific binding was determined with the addition of 1 μM ryanodine. Tests were run in triplicate and concentration-responses were conducted at least twice using different JSR preparations.

RyR1 single channel recordings in planar lipid bilayer. Single channel recordings were completed following previously described methods (Pessah *et al.*, 2009). Briefly, measurements of single RyR1 channels were conducted by inducing JSR vesicle fusion with BLM; composed of 30 mg/ml phosphatidylethanolamine, phosphatidylserine, and phosphatidylcholine in *n*-decane (Avanti). A 10:1 cytoplasmic (*cis*) to lumen (*trans*) side chemical gradient of Cs^+ was built by 500–50 mM of CsCl, buffered with 20 mM HEPES, pH 7.4. Channel currents were recorded at a holding potential of −40 mV applied to the *trans* lumen side that had 100 μM Ca^{2+}. JSR vesicles (1–4 μg/ml), test PCBs, and defined free Ca^{2+} (2 μM) were introduced to the *cis*-cytosolic channel face, which served as virtual ground. Prior to the addition of a given treatment, baseline recordings (control) were acquired for approximately 60 s. After baseline recordings, chemical treatments were added to the channel sequentially and channels monitored extended periods of time that lasted up to 5 min after the addition of varying PCBs or PCB concentrations. Thus, chemical exposure could be compared directly to a given channels' baseline gating behavior. Recordings in the presence of DMSO tested up to 1% (v/v) showed negligible changes in channel gating (data not shown and see O'Neill *et al.*, 2003) and in the current study never exceeded 0.5% (v/v). Data acquisition was made through Digidata 1440A (Axon-Molecular Devices), digitized at 10 kHz after 1 kHz low-pass filter (Low-Pass Bessel Filter 8 Pole). A schematic graph briefly depicting the process is shown in the Figure 3A.

Statistics and data analysis. For [^{3}H]Ry binding assays, specific binding was calculated by subtracting the nonspecific binding from the observed total binding as measured in disintegrations per minute (DPM). Concentration responses were tested in at least 2 different JSR preparations ($n \geq 2$) and each concentration was run in triplicate per experiment (3 technical replicates). Under these analyses, assuming 80% power and an $\alpha \leq 0.05$, $n = 2$ would detect a difference of 200 DPM (Minitab; SD = 36; geometric mean of the SD observed in DMSO controls; where DMSO controls were run with every congener each experiment). This change in DPM would be approximately 136% change in

[^{3}H]Ry binding compared with the DMSO control (assuming mean = 560 DPM; geometric mean of the average DPM for the DMSO controls).

Concentration response curves were created using specific binding normalized to the DMSO control from the same experiment and displayed as a percent. Percent responses were fit to sigmoidal concentration-response curves (PRISM 6.0) that were used to estimate maximal percent activation, the effective concentration causing 50% of maximal response (EC_{50}), and the concentration that would cause a 200% over activation of the receptor (EC_{2X}). Nonlinear regression models had ≥ 32 degrees of freedom for goodness of fit assessments. To evaluate the predictions of previously developed QSAR (Rayne and Forest, 2010), the predicted versus experimental log-EC_{2x} were compared via Pearson's correlation. Inactive or low efficacy congeners, as determined in [^{3}H]Ry binding assays, were ascribed an EC_{2x} of 30 μM to remain consistent with the concentration range utilized in the developed QSAR (Rayne and Forest, 2010), which predicted that only 14 congeners would completely lack RyR activity.

Single channel recording data was analyzed using pClamp 10.4 (Molecular Devices); where recorded traces were analyzed for channel open probability (P_O) and current amplitude distribution. Open probability represents the ratio of time that the channel spends in the open state (τ_O) relative to the dwell time in the closed state (τ_C). The baseline gating activity of each reconstituted channel was recorded for approximately 1 min followed by the sequential addition of PCB 202, PCB 197, or PCB 11 from low to high concentration. Channel gating activity for each PCB at a given PCB concentration was recorded for an extended period of time that was up to 5 min after chemical addition. Thus, chemical affects were determined relative to the respective baseline recording. For PCB 202, affects between 100 nM to 10 μM were conducted on a single channel recorded for prolonged periods of time under baseline or a given PCB 202 concentration. Time periods of the channel recording under the baseline or chemical treatments were then compared using a repeated measures analysis of variance (ANOVA; Origin 9.0) and differences between treatments compared using a Tukey's *post-hoc* analysis. This method was used to determine the lowest concentration of PCB 202 that would cause the maximum change in receptor gating kinetics. Once determined, the lowest maximal effect concentration (see results; 200 nM PCB 202; Figure 3) was assessed in 6 individual RyR1 channels and compared with kinetics in the presence of picomolar concentrations of PCB 202 ($n = 6$). Similarly, the effect of PCB 197 were assessed in multiple individual channels at 200 pM ($n = 3$) and 200 nM ($n = 4$). Here, the P_o in the presence of PCB 202 or PCB 197 in the pM–nM range were normalized to their respective baseline and significance determined using a paired sample *t*-test. The pairwise SD was 39.5% for PCB treatment relative to the baseline control, where assuming 80% power and an $\alpha \leq 0.05$, a $n = 6$ would detect a difference of 56% from the baseline (eg, 100% compared with 156% increase in P_O). An $n = 3$ would detect a difference of 128.9% compared with baseline (eg, 100–228.9%).

RESULTS

Predicted Versus Experimental Activity of PCBs Towards RyR1

We assess the RyR-based toxicity of 14 PCB congeners that have not previously been assessed for channel activity (Table 1A), expanding our previous SAR (Pessah *et al.*, 2006). We also re-assessed the binding activity of previously published congeners (Pessah *et al.*, 2006) and demonstrated high reproducibility of the [^{3}H]Ry binding assay (Table 1B). Of the 14 congeners tested in [^{3}H]Ry binding assays, 11 PCBs were found to cause a 200%, or greater, overactivation (EC_{2X}) of the RyR. Together with previous work this brings the total number of active RyR congeners to 42, out of the 49 congeners that have been tested to date (current work and Pessah *et al.*, 2006). Maximum effects and effective concentrations for all congeners are summarized in Table 1 and are shown next to their corresponding predicted (Table 1A) or previously published EC_{2X}.

Tetra-*ortho* PCB 202, lacking *para*-substitution, displayed the highest RyR1 potency of the congeners assessed with an EC_{2x} of 0.05 μM in [^{3}H]Ry binding assays (Figure 1 and Table 1A). The finding that PCB 202 is the most potent RyR PCB congener agrees with the predictions of the QSAR by Rayne and Forest (2010) but we demonstrate a higher potency than the QSAR predicted (Table 1A). The concentration response curves for PCB 202 compared with PCB 95, 194, and 197 can be found in Figure 1 and are displayed in different panels to help demonstrate the differences in RyR-activation curves by these structurally distinct congeners. When compared with PCB 95, a tri-*ortho* PCB previously suggested in experimental assessments as the most potent RyR congener, PCB 202 displayed an almost 2-fold higher apparent potency, but lower efficacy (maximum response; Figure 1 and Table 1A and B). When PCB 202 is compared with PCB 194 and PCB 197, all containing 8 chlorine substitutions, the importance of *meta*-substitution adjacent to the *ortho*-chlorines is clearly demonstrated. PCB 194, lacking 6,6′*ortho*-chlorines but containing both 5,5′ *meta*-substitutions, is highly efficacious and potent displaying an EC_{2X} of 0.07 μM and causing a maximum

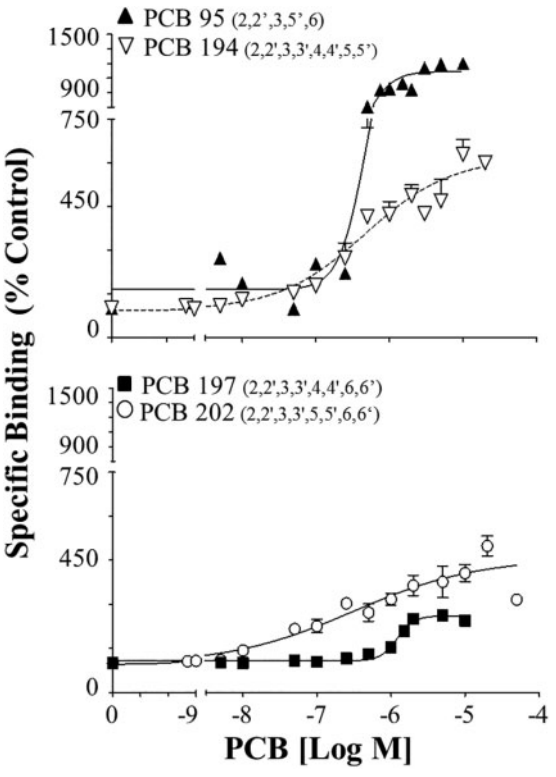

FIG. 1. Binding of [^{3}H]Ry to the RyR1 in the presence of PCB 202 in comparison to PCB 95, 194, and PCB 197 to demonstrate the importance of *ortho*, *meta*, and *para*-chlorine substitutions. Specific binding is shown relative to DMSO control (100%). Congeners were placed in different panel to aid visualization. Concentration response curves were assessed using nonlinear regression. Numbers represent Mean ± SEM; from 2 protein preparations ($n \geq 2$) where each treatment was run in triplicate for each protein preparation.

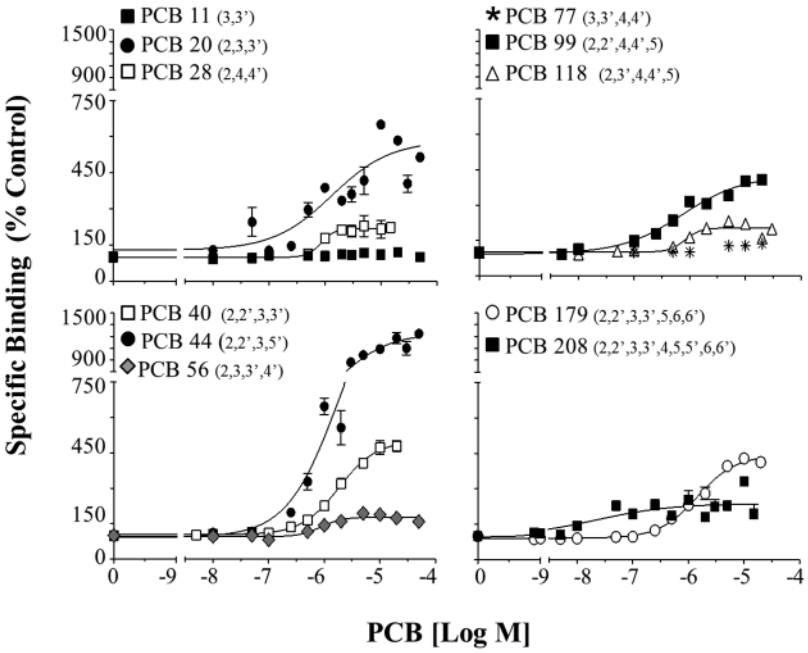

FIG. 2. Concentration response curves for the remaining 11 PCB congeners tested for the first time in the current study for RyR binding activity. Specific binding is shown relative to DMSO control (100%). RyR1 activity of the different PCB congeners is shown in different panels based on chlorine number to aid visualization. Concentration response curves were assessed using nonlinear regression. Numbers represent Mean ± SEM; from 2 protein preparations ($n \geq 2$) where each treatment was run in triplicate for each protein preparation.

618% overactivation of the channel. Conversely, tetra-*ortho* PCB 197, which lacks the 5,5′ *meta*-substitution pattern and contains *para*-substitution, shows ~35-fold lower EC_{2X} of 1.76 μM and nearly 2-fold lower maximum response at just 261% overactivation of the channel.

Additional concentration response curves for the remaining 11 PCBs that were tested for the first time in the current study can be found in Figure 2 and are separated into separate panels based on chlorine number to aid visualization. One pattern that can be seen in Figure 2 is the impact of *para*-substitution on the RyR-activity of different PCBs; for example when comparing the tri-*ortho* congeners PCB 44 and PCB 99. Both congeners activate the channel but PCB 44, without *para* substitution, displays a 3-fold great maximum efficacy and an approximate 2-fold higher potency compared with PCB 99, which has both *para* positions occupied (Table 1A and Figure 2). It should be noted however that the 95% confidence intervals for the PCB 44 and PCB 99 EC_{2X}'s overlap. The non- and mono-*ortho*-substituted congeners tested in the current study displayed little to no RyR activity (Table 1A and Figure 2). This included non-*ortho* congeners PCB 11, which caused no activation, and PCB 77 that unexpectedly caused a slight activation of the RyR (maximum 130%) at concentrations higher than 10 μM. Mono-*ortho* congeners tested included PCB 20, 28, 56, and 118. Of the mono-*ortho* congener PCB 20 (chlorines in the 2, 3, 3′ position) displayed a high potency and efficacy ($EC_{2X} = 0.25$; 570% maximum overactivation) and was more RyR-active than the mono-*ortho* congeners containing *para* substitution (ie, PCB 28, 56, and 118). These findings support a minimal mono-*orthro* substitution for RyR-activity and that congeners with *ortho*-substitution in the presence of *para*-substitution will likely display lower RyR activity than similar chlorine substituted congeners lacking *para*-substitution.

The RyR1 based NDL PCB QSAR (Rayne and Forest, 2010) displayed a moderate predictive capability, such that, the predictive and experimentally derived EC_{2X} values were significantly correlated ($r = 0.71$; $P = 0.004$, Supplementary Fig. 5). When the experimental versus predictive EC_{2X} values of single congeners are compared (Table 1A) the experimental measurements describe receptor activation occurring at lower concentrations. Several exceptions included PCB 179 and 197, both displaying effective concentrations at higher concentrations than predicted by the QSAR. The QSAR model suggested that the *ortho*-substitution number was, in large part, driving potency at the RyR1 (Rayne and Forest, 2010) but both PCB 179 and PCB 197 have 4 *ortho*-substitutions but lack one or both chlorines in the *meta* position, respectively. These findings support the importance of chlorines in the *meta* position, in addition to the *ortho* position, for PCB congener activity at the RyR.

NDL PCBs Alter RyR1 Single Channel Gating Behavior

[^{3}H]Ry binding assay revealed drastic differences in the RyR-activity of PCB 202 and PCB 197 (Figure 1 and Table 1A, EC_{2X} 50 nM and 1.76 μM, respectively). Both PCB 202 and PCB 197 are tetra-*ortho* congeners with 8 total chlorines but PCB 202 lacks *para*-substitution and PCB 197 lacks *meta*-substitution but contains *para*-substitutions. Due to these distinct potency differences, especially in light of structural similarities and differences, these congeners were chosen for further evaluation in single channel gating analysis in comparison to non-*ortho* PCB 11, which was completely inactive in [^{3}H]Ry binding assays.

Figure 3A shows a schematic graph depicting the recording process of an incorporated RyR1 channel in BLM and representative traces of RyR1 at baseline or in the presence of increasing concentrations of PCB 202 can be found in Figure 3B. Overall, Figure 3 shows that PCB 202 concentrations between 100 nM and 10 μM caused significant changes in the open probability (P_o) of RyR1 compared with the baseline (control) conditions (Figure 3C; repeated measures ANOVA; $P \leq 0.0001$). Specifically, starting at 100 nM, addition to the *cis*-side of the channel, PCB

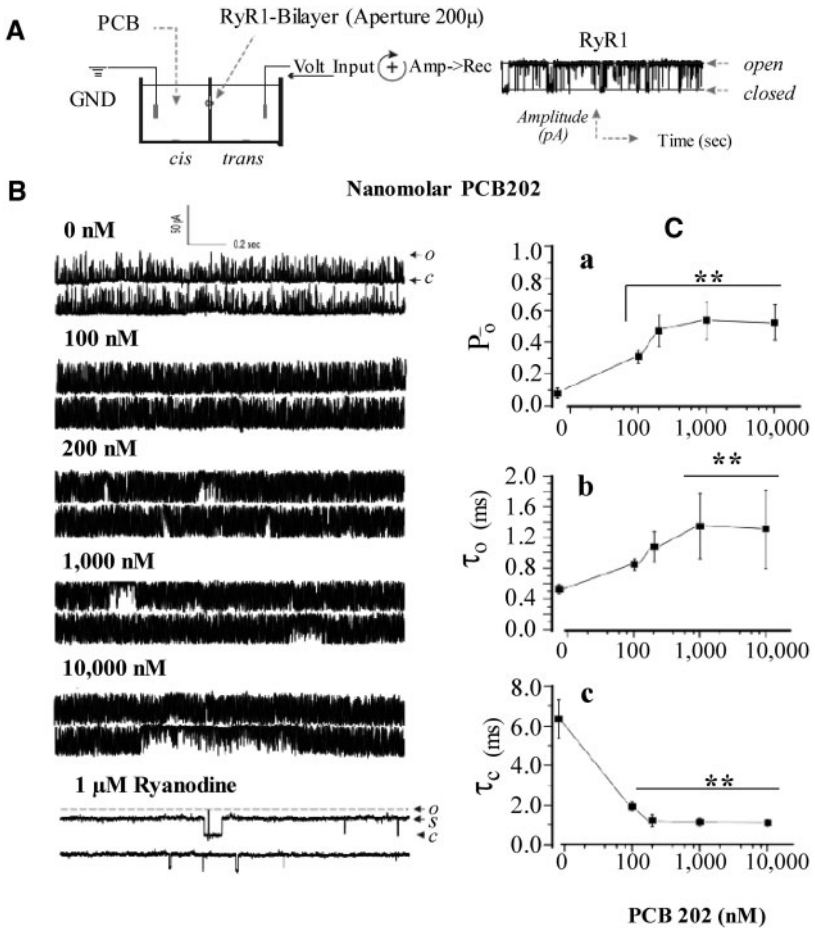

FIG. 3. PCB 202 influences RyR1 channel gating kinetics in a concentration-dependent manner. (A) Schematic diagram of the RyR1 channel reconstitution across the BLM chamber. (B) Representative traces of single RyR1 channel gating activity before and after stepwise increase in PCB 202 concentrations. Recordings of channel gating activity were measured for several minutes before the sequential addition of PCB 202 on the cis (cytoplasmic) side of the RyR1 channel. Traces shown are representative sections of the RyR1 channel. (C) Concentration-dependent change in open probability (P_o, a) and corresponding changes in the mean open dwell time (τ_o, b) and the mean closed time (τ_c, c). Channel kinetic data in (C) are the Mean ± SD from 4 different recording time periods (eg, parameter during the initial 20 s exposure to given treatment). Abbreviations: Ground (GND), polychlorinated biphenyl (PCB), cytoplasmic side (*cis*), luminal side (*trans*), voltage input (volt-input), amplifier to recorded (Amp -> Rec), open channel state (O); closed channel state (C); sub-conductance state (S). Differences indicated in panel (C) were assessed using repeated measures ANOVA with a Tukey *post-hoc* analysis. **$P \leq .01$ relative to the control; †$P \leq .05$ relative to PCB 202 at 100 nM. $n = 4$ time periods.

202 caused a significant increase in the P_o of the RyR channel (traces Figure 3B) that was approximately 300% greater than baseline conditions. The increase in P_o was due to an increased trend in the mean open dwell time (τ_O) and a significant decrease in the mean closed dwell time (τ_C) (see Figure 3C: (a) P_o, (b) τ_O, and (c) τ_C). Subsequent sequential additions of PCB 202 to a final concentration 200 nM caused a greater increase in the P_O of the RyR1 channel due to further increased τ_O and decreased τ_C (Figure 3C). Further escalation of PCB 202 concentrations in the *cis* chamber (1–10 μM) did not cause additional changes to the gating kinetics of the RyR1-channel. Final addition of the ligand ryanodine (1 μM) to the PCB 202 modified channel was able to lock the channel into the characteristic long-lasting sub-conductance state as anticipated from previous studies. This demonstrates saturability with the maximum increase in PCB 202-induced channel P_o observed at just 200 nM and that PCB 202 induced changes in P_O are specifically due to increased time in the open state in combination with shorter-lived transitions in the closed state.

We then aimed to determine the threshold concentration of PCB 202 that could cause a statistically significant change in RyR1 gating. PCB 202 as low as 200 pM induced changes in RyR1 channel gating kinetics (Figure 4A; representative traces) characterized by a significant right-shift in the current frequency histogram (Figure 4B). The change in current amplitude distribution was consistent with a significantly increased P_o as compared with the channel's baseline behavior before exposure to PCB 202 (Figure 4C). Here, PCB 202 caused an approximate 200% increase in P_o compared with baseline recordings and these findings were consistent in 6 independently recorded channels (Mean P_o = 199.0% compared with baseline; pairwise SD = 39.5%; paired sample *t*-test, $P \leq .001$). The magnitude of channel activation by PCB 202 as seen in both the current amplitude distribution and the channel's P_o was concentration dependent (compare 200 pM vs 200 nM).

Consistent with [^{3}H]Ry binding results, PCB 197 displayed a much lower potency in single-channel recordings as compared with PCB 202. PCB 197 at 200 pM did not have detectable influence (representative traces not shown) on channel gating activity, where neither channel current amplitude distributions (Figure 4B) nor P_o (Figure 4C) were significantly different from the baseline recording period. Overall, 200 nM of PCB 197 was required to appreciably shift channel current amplitude distributions and channel current amplitudes to a level similar to

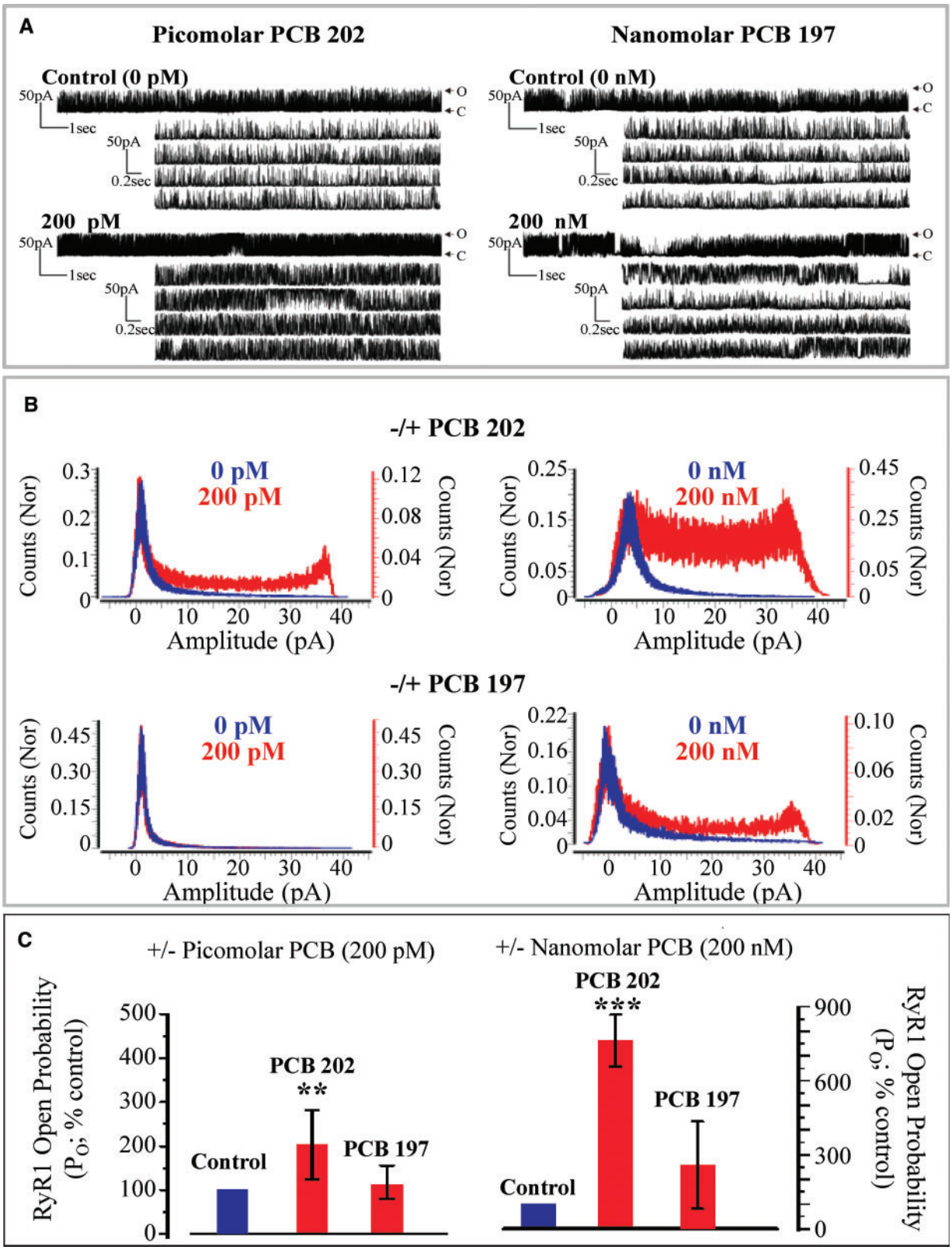

FIG. 4. Comparison of RyR1 channel gating behavior in the presence of PCB 202 or PCB 197 at 200 pM or 200 nM. (A) Representative traces of (PCB 202 and PCB 197 at 200 pM or 200 nM, respectively). Note PCB 202 at 200 nM and PCB 197 at 200 pM traces are not shown for space purposes. Abbreviations: open channel state (O); closed channel state (C). (B) Frequency histograms of the RyR1 channel current amplitudes before (Blue) and after (Red) addition of PCBs. Bin width 0.1 pA, Y-axis are the normalized (Nor) counts relative to number of events. (C) Percent changes in the open probability (P_o) of the PCB exposed channel relative to the P_o under baseline (control) conditions. Mean ± SD; PCB 202 $n = 6$; PCB 197 at 200 pM $n = 3$ and PCB 197 at 200 nM $n = 4$,***$P \leq .001$ relative to baseline (100%) as determined with a paired sample t-test. (Full color version available online).

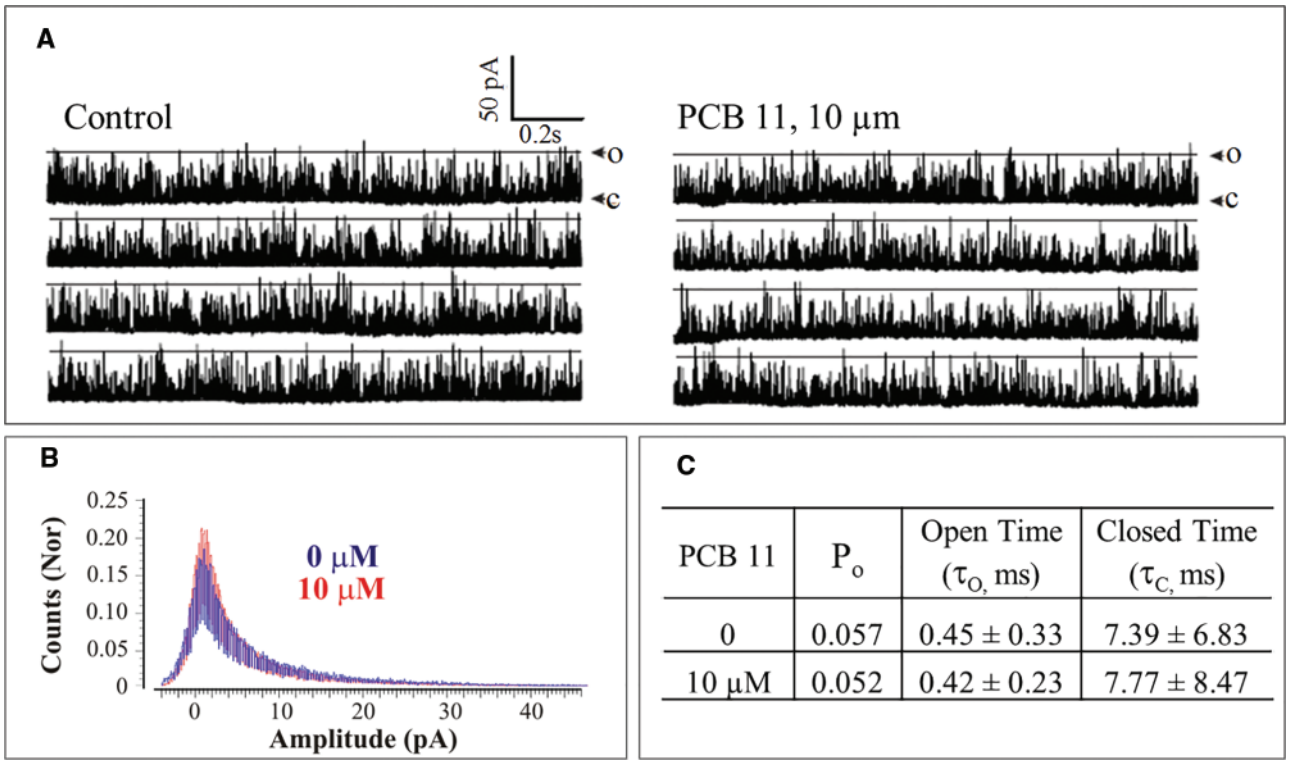

FIG. 5. Analysis of single RyR1 channel gating behavior before and after exposure to PCB 11 on the cytoplasmic side of the channel. (A) Representative traces at baseline and in the presence of PCB 11. Abbreviations: open channel state (O); closed channel state (C). (B) Frequency histograms of the RyR1 channel current amplitudes before (Blue) and after (Red) addition of PCB 11. Bin width 0.1 pA, Y-axis are the normalized (Nor) counts relative to number of events. (C) Summary analysis of kinetic parameters for the channel shown in panel A in the absence or presence of PCB 11: the open probability (P_o), mean open dwell time (τ_o), and mean closed dwell time (τ_C). This experiment was replicated twice with similar results. (Full color version available online).

that produced by 200 pM PCB 202 (Figure 4C). Here, PCB 197 caused a mean change in P_o of 350% as compared with the baseline P_o. There was a large amount of variability in the change induced by PCB 197 at 200 nM (Mean P_o= 353.6%; pairwise SD = 259.3%; paired sample *t*-test; $P = .15$).

As demonstrated in [^{3}H]Ry binding assays, PCB 11 at 10 µM did not affect channel P_o (103% of baseline activity; $n = 2$; Figure 5). To further confirm lack of RyR activity, we measured the influence of PCB 11 on macroscopic Ca^{2+} fluxes across microsomes enriched in SERCA pumps and RyR1 channels, which act dynamically to accumulate and release Ca^{2+} across the microsomal vesicles. As shown in Supplementary Figure 6, after the Ca^{2+} loading phase of 3 sequential additions of 45 nmol Ca^{2+} to each cuvette (Supplemental Methods), the addition of DMSO or PCB 11 did not trigger release of accumulated Ca^{2+} by the vesicles in the presence of SERCA activity. PCB 95, a RyR1 activator, and ruthenium red, a RyR1 blocker, were then added to the DMSO cuvette as a positive and negative control for RyR1 function, respectively. The QSAR predicted that PCB 11 would have minimal RyR-activity (predicted EC_{2X} of ~10 µM) but with the current findings PCB 11 would be considered inactive supporting a minimal mono-*ortho* substitution for RyR activity.

DISCUSSION

The current study expanded and supported the SAR for NDL PCBs towards the RyR, an important target linked to neurotoxicity. We demonstrate that *in vitro* [^{3}H]Ry-binding assays are highly reproducible and likely act as conservative measures of RyR-activation. Specifically, we found that pM levels of PCBs can alter receptor channel gating behavior. So far, 49 of the 209 PCB congeners have been tested for RyR activity. Of the 49 tested, 42 alter RyR activity (current work and Pessah *et al.*, 2006); however; the total number of PCBs, and other noncoplanar compounds, including PBDEs and hydroxylated-PCBs (Fritsch and Pessah, 2013; Kim *et al.*, 2010; Niknam *et al.*, 2013), that could contribute to RyR mediated toxicity in environmental mixtures, is probably higher (Rayne and Forest, 2010). Work suggests that RyR-active PCBs and PBDEs display additivity at the receptor (Fritsch and Pessah, 2013; Kostyniak *et al.*, 2005; Pessah *et al.*, 2006) demonstrating that the Ca^{2+} channel is likely a common target of contaminants mixtures currently found in the environment.

The prediction of the QSAR developed by Rayne and Forest (2010) were supported in the current study. Tetra-*ortho* PCB 202 was found to be the most potent congener identified to date instead of the previously recognized tri-*ortho* PCB 95. However, RyR1 mediated toxicity is differentially affected by PCB enantiomers (Pessah *et al.*, 2009). There are 19 chiral PCBs, including PCB 95, and thus 1 enantiomer of PCB 95 may display a greater potency toward the RyR then that of the nonchiral PCB 202. The current work also demonstrated higher potency than that outlined by QSAR predictions suggesting that the QSAR predictions may act as a conservative measure of PCB mixture toxicity. Several congener's experimental potencies did not match QSAR predictions, including PCB 179 and 197 which both displayed lower potency than predicted. It is suggested that too much emphasis may have been placed on *ortho* substitution because the QSAR predicted that potency was directly related to chlorine number whereby higher chlorinated congeners automatically

have more *ortho* substitution (Rayne and Forest, 2010). Experimental data demonstrate the importance of *ortho* with adjacent *meta*-substitution (eg, PCB 194 vs PCB 197, Figure 1) and a new QSAR with emphasis on chlorines in both positions may provide even more predictive potency values.

The SAR for RyR active PCBs developed using [^{3}H]Ry binding assays is consistent with the SAR observed in single channel voltage clamp analysis, demonstrating the predictive power of the SAR found in [^{3}H]Ry binding assays. However, whereas the SAR was consistent our findings suggest that the [^{3}H]Ry binding assay significantly underestimates the true potency of NDL PCBs towards RyR because the 2 assays demonstrated different sensitivities to NDL PCBs. The difference in potency; 200 pM or 50 nM of PCB 202 altered receptor gating or receptor ligand binding, respectively, may be due to the different endpoints being measured. The [^{3}H]Ry binding analysis represents the activity of the receptors in a tissue extract after reaching saturation but BLM recording represents activation and monitoring of a single channel in real-time. [^{3}H]Ry binding assessments also contain more microsomal lipid in the aqueous assay, which would appreciably reduce the free PCBs. In single channel voltage clamp the total lipid composition would be at least 6- to 24-fold lower (JSR concentrations; 24 μg/ml in [^{3}H]Ry assays vs 1–4 μg/ml in BLM) presenting an insignificant effect on NDL PCB concentration when introduced to the cytoplasmic side of the channel.

The findings that NDL PCBs increase the open probability of the RyR are consistent with previous studies with NDL PCBs and other RyR-active compounds, namely Bastadin 10 (Chen *et al.*, 1999; Pessah *et al.*, 2009; Samsó *et al.*, 2009). But in the current study we show that much lower, environmentally relevant, concentrations of PCBs could lead to distinct changes in the gating behavior and functional regulation of RyR channels (Niknam *et al.*, 2013; Pessah *et al.*, 2009). Currently the direct site(s) of interaction between the RyR and NDL PCBs is unknown but it is thought to be within the FKBP12–RyR1 interaction domain because NDL PCB-induced RyR activity can be eliminated by pretreatment with the immunophilin drugs FK506 and rapamycin (Wong and Pessah, 1997). The FK506 binding protein 12 kDa (ie, FKBP12) is an accessory protein that stabilizes the conformational state of the RyR. Disruption of the FKBP12–RyR complex, through genetic or pharmacological manipulation, causes an increase in channel open probability and causes the channel to exhibit a sub-conductance state, or conductance below the channel's maximum conductance, that leaks Ca^{2+} (Ahern *et al.*, 1997; Bellinger *et al.*, 2008; Zalk *et al.*, 2007). Thus, it is suggested that the increased open probability caused by NDL PCB toxicity at the RyR would lead to channels that leak Ca^{2+} from the SR/ER stores due to the disrupted FKBP12–RyR complex and the changes in intracellular Ca^{2+} would contribute to altered neuromuscular function.

The current work focused on NDL PCB-activation of RyR1 using skeletal muscle preparations. Skeletal muscle may be a target of NDL PCB toxicity at the RyR (Niknam *et al.*, 2013) but developmental neurotoxicity has arisen as the prime toxic outcome of concern for NDL PCB exposure. Here, we use the skeletal muscle as a model for NDL PCBs on neuronal systems because (1) it represents a large source of primarily 1 RyR channel, namely, RyR1, eliminating potential differences in concentration responses due to the presence of multiple channel types as seen in neuronal tissue, (2) RyR1 is highly expressed in the brain, (3) NDL PCB toxicity at the so-called cardiac isoform, RyR2, also highly expressed in the brain, follows the same SAR (Pessah *et al.*, 2010), and (4) the impact of NDL PCBs on dendritic growth in cultured hippocampal neurons can be eliminated by siRNA knockdown of either RyR1 or RyR2 (Wayman *et al.*, 2012b). NDL PCB activity at the RyR also follows the same SAR in different regions of the brain (Wong *et al.*, 1997) but potency values were reported in the micromolar range. The difference in potency, as compared with the pM–nM range reported here, may be due to drastic differences in assay conditions. Specifically, Wong *et al.* (1997) used crude microsomal preparations, that were not purified through a differential sucrose gradient as in the current study, and [^{3}H]Ry binding assays contained ~700 μg/ml of protein. The [^{3}H]Ry binding assays in the 1997 publication also utilized 10 μM $CaCl_2$, versus 50 μM in the current study, where the RyR channel's open state is highly sensitive to buffer Ca^{2+} levels (Pessah *et al.*, 1987). Further assessments addressing NDL PCB activity at the RyR in different regions of the brain, but under the current [^{3}H]Ry binding conditions, would strengthen the connection between the current SAR and predictions of neurotoxic risk. However, research has demonstrated that pM to low nM PCB 95 can alter dendritic growth in cultured hippocampal neurons (Wayman *et al.*, 2012b; Yang *et al.*, 2009) supporting the pM to nM toxicity range demonstrated in the current study.

Additional studies provide evidence that RyR *in vitro* toxicity could contribute to *in vivo* neurotoxic outcomes. Organisms exposed during development to PCB 95 and Aroclor 1254, a mixture with increased *ortho*-substituted PCBs, have altered dendritic arborization in the hippocampus (Yang *et al.*, 2009) and altered RyR1 and RyR, isoform 2 (RyR2) expression in their cerebellum. In these studies, the exposed animals had altered learning and had PCB congeners in their brains that consisted of numerous RyR active congeners including PCB 99, 153, 170, 180, 183, and 187 but did not contain PCB 77, 126, and 169 (Yang *et al.*, 2009). Another study with weanling mice exposed to a mixture of PCB 28, 52, 101, 138, 153, and 180 through lactation displayed age specific disruption in motor function and persistent anxiety like behavior (Elnar *et al.*, 2012). These PCBs all display RyR activity and the weanlings displayed anxiety likely behavior that was correlated with the expression of RyR, isoform 3.

Polychlorinated biphenyls (PCB) concentrations found in human samples have also been correlated with cognitive or behavioral deficits in adults (Fitzgerald *et al.*, 2008; Schantz *et al.*, 2001) and children (Jacobson and Jacobson, 1996; Lonky *et al.*, 1996; Stewart *et al.*, 2008). Deficits in children have included lowered IQ scores, impaired learning and memory, and attention deficit (Jacobson and Jacobson, 1996; Lonky *et al.*, 1996; Stewart *et al.*, 2008). It is well recognized that PCB residues in these samples are complex mixtures but neurotoxic outcomes due to PCB mixture exposure have been largely ascribed to NDL congeners because they are found in relatively high concentrations in the brains of human and experimental animals that display neuropsychological deficits (Mitchell *et al.*, 2012; Pessah *et al.*, 2010) NDL PCBs also constitute the majority of the total PCB burden in both human and environmental samples (Hwang *et al.*, 2001, 2006; Marek *et al.*, 2013; Stahl *et al.*, 2009) and further understanding the contribution of the RyR, alone or in combination with other modes of NDL PCB neurotoxicity (see "Introduction" section), would help further elucidate risks in human populations.

In addition to NDL PCB induced neurotoxicity, enhanced RyR activity has implications on the health and performance of non-neuronal systems (Niknam *et al.*, 2013; Pessah *et al.*, 2010). The RyR was first identified and characterized for its role in excitation-contraction coupling (EC) (Pessah *et al.*, 1985), which is essential to the normal function of both cardiac and skeletal

muscle. NDL PCBs disrupt important aspects of EC coupling in exposed skeletal myotubes demonstrating a direct impact on muscle performance (Niknam *et al.*, 2013). The cardiac RyR-isoform, RyR2, is also sensitive to NDL PCBs (Pessah *et al.*, 2009) but whether NDL PCB activity at RyR2 causes cardiac EC-coupling dysfunction requires further elucidation. Such studies may help explain the observed effects of PCB exposure that has been associated with an increase in cardiac physiological dysfunction (Bergkvist *et al.*, 2015). Finally, the RyR and related Ca^{2+} signaling proteins have been demonstrated to have roles in diseases ranging from cardiac arrhythmias (Lacampagne *et al.*, 2008) and malignant hypothermia (Robinson *et al.*, 2006) to Alzheimer's disease (Bruno *et al.*, 2012; Stutzmann *et al.*, 2006) and autism spectrum disorder (Pessah *et al.*, 2010; Shelton *et al.*, 2012; Stamou *et al.*, 2013). Currently, it is unclear whether NDL PCB toxicity at the RyR may contribute to these disease states but the potential gene by environment interaction warrants further investigation.

CONCLUSION

As evidence regarding the impact of NDL PCBs mounts, numerous research groups have started developing and applying new risk assessment tools to define NDL PCB neurotoxic risk. This includes the development of a relative potency scheme called the neurotoxic equivalency (NEQ) scheme. The NEQ is similar to and would complement the well-known TCDD equivalency scheme (TEQ), commonly used to assess PCB mixture toxicity. Whereas still in its infancy, the NEQ faces several challenges before establishment in risk assessment. First, numerous modes of neurotoxicity have been documented (see "Introduction" section), often displaying different SAR requirements (eg, current work and Stenberg *et al.*, 2011), and the question arises regarding what modes and how many modes should be included to establish an NEQ. To date the RyR is the most sensitive target of NDL PCBs and has been included in the development of NEQ schemes (Rayne and Forest, 2010; Simon *et al.*, 2007). Additionally, few congeners have been tested in the various neurotoxic assays; making QSAR studies essential. Here, we evaluated and supported the predictions of a RyR-based neurotoxic QSAR that has been used to define NEQs for NDL PCBs (Rayne and Forest, 2010). As predicted, PCB 202 is a highly RyR potent PCB congener, and whereas it is detected in human and environmental samples, it likely does not represent a large percentage of total PCB burdens (Marek *et al.*, 2013; Stahl *et al.*, 2009). However, similar to TCDD in the TEQ scheme, PCB 202 could act as a reference compound for which PCB mixture toxicity toward the RyR is based. Therefore, additional *in vitro* and *in vivo* assessments, focused specifically on PCB 202, could provide valuable information for understanding or further modeling NDL PCB mixture induced neurotoxicity and these efforts would further establish the NEQ for application in risk assessment.

SUPPLEMENTARY DATA

Supplementary data are available online at http://toxsci.oxfordjournals.org/.

ACKNOWLEDGMENT

The content is solely the responsibility of the authors and does not necessarily represent the official views of NIH or USEPA. The authors declare no competing financial interests.

FUNDING

National Institute of Environmental Health Sciences (NIEHS) Superfund Research Program at UC Davis (INP and EBH; P42-ES004699); Iowa Superfund Research Program (HJL; P42-ES013661); National Heart Lung and Blood Institute (EBH; UC Davis T32-HL086350); NIEHS (1R01-ES014901, 1R01-ES017425); the UC Davis Center for Children's Environmental Health (1P01-ES011269); U.S. Environmental Protection Agency through the Science to Achieve Results Program Grant (Nos. R829388 and R833292); IDDRC Core Center U54 HD079125.

REFERENCES

Ahern, G. P., Junankar, P. R., and Dulhunty, A. F. (1997). Subconductance states in single-channel activity of skeletal muscle ryanodine receptors after removal of FKBP12. *Biophys. J.* **72**, 146.

Bell, M. R. (2014). Endocrine-disrupting actions of PCBs on brain development and social and reproductive behaviors. *Curr. Opin. Pharmacol.* **19**, 134–144.

Bellinger, A. M., Mongillo, M., and Marks, A. R. (2008). Stressed out: The skeletal muscle ryanodine receptor as a target of stress. *J. Clin. Investig.* **118**, 445–453.

Bergkvist, C., Berglund, M., Glynn, A., Wolk, A., and Åkesson, A. (2015). Dietary exposure to polychlorinated biphenyls and risk of myocardial infarction—A population-based prospective cohort study. *Int. J. Cardiol.* **183**, 242–248.

Berridge, M. J. 2012. Cell signaling pathways—Module 2. *Cell Signal. Biol.* **2**, 1–130.

Boix, J., Cauli, O., Leslie, H., and Felipo, V. (2011). Differential long-term effects of developmental exposure to polychlorinated biphenyls 52, 138 or 180 on motor activity and neurotransmission. Gender dependence and mechanisms involved. *Neurochem. Int.* **58**, 69–77.

Bruno, A. M., Huang, J. Y., Bennett, D. A., Marr, R. A., Hastings, M. L., and Stutzmann, G. E. (2012). Altered ryanodine receptor expression in mild cognitive impairment and Alzheimer's disease. *Neurobiol. Aging* **33**, 1001.e1001–1001.e1006.

Chen, L., Molinski, T. F., and Pessah, I. N. (1999). Bastadin 10 stabilizes the open conformation of the ryanodine-sensitive Ca2^{+} channel in an FKBP12-dependent Manner. *J. Biol. Chem.* **274**, 32603–32612.

Choi, S. Y., Lee, K., Park, Y., Lee, S. H., Jo, S. H., Chung, S., and Kim, K. T. (2016). Non-dioxin-like polychlorinated biphenyls inhibit G-protein coupled receptor-mediated Ca^{2+} signaling by blocking store-operated Ca^{2+} entry. *PloS One* **11**, e0150921.

Dickerson, S. M., Guevara, E., Woller, M. J., and Gore, A. C. (2009). Cell death mechanisms in GT1-7 GnRH cells exposed to polychlorinated biphenyls PCB74, PCB118, and PCB153. *Toxicol. Appl. Pharmacol.* **237**, 237–245.

Domingo, J. L., and Bocio, A. (2007). Levels of PCDD/PCDFs and PCBs in edible marine species and human intake: A literature review. *Environ. Int.* **33**, 397–405.

Elnar, A. A., Diesel, B., Desor, F., Feidt, C., Bouayed, J., Kiemer, A. K., and Soulimani, R. (2012). Neurodevelopmental and behavioral toxicity via lactational exposure to the sum of six indicator non-dioxin-like-polychlorinated biphenyls (∑6 NDL-PCBs) in mice. *Toxicology* **299**, 44–54.

Faroon, O., and Ruiz, P. 2015. Polychlorinated biphenyls: New evidence from the last decade. *Toxicol. Ind. Health*. doi: 10.1177/0748233715587849.

Fernandes, E. C. A., Hendriks, H. S., van Kleef, R. G., Reniers, A., Andersson, P. L., van den Berg, M., and Westerink, R. H. (2010). Activation and Potentiation of Human GABAA Receptors by Non-Dioxin–Like PCBs Depends on Chlorination Pattern. *Toxicol. Sci* **118**, 183–190.

Fitzgerald, E. F., Belanger, E. E., Gomez, M. I., Cayo, M., McCaffrey, R. J., Seegal, R. F., Jansing, R. L., Hwang, S., *et al.* (2008). Polychlorinated biphenyl exposure and neuropsychological status among older residents of upper Hudson River communities. *Environ. Health Perspect* **116**, 209.

Fonnum, F., and Mariussen, E. (2009). Mechanisms involved in the neurotoxic effects of environmental toxicants such as polychlorinated biphenyls and brominated flame retardants. *J. Neurochem.* **111**, 1327–1347.

Frame, G. E. 2001. The curent state-of-the-art of comprehensive, quantitative, congener-specific PCB analysis, and what we now know about the distribution of individual congeners in commercial aroclor mixtures. In *PCBs, Recent Advances in Environmental Toxicology and Health Effects* (L. G. Hansen, L. W. Robertson, Eds.). University Press of Kentuky, Lexington.

Fritsch, E. B., and Pessah, I. N. (2013). Structure–activity relationship of non-coplanar polychlorinated biphenyls toward skeletal muscle ryanodine receptors in rainbow trout (*Oncorhynchus mykiss*). *Aquat. Toxicol.* **140–141**, 204–212.

Gafni, J., Wong, P. W., and Pessah, I. N. (2004). Non-coplanar 2,2′,3,5′,6-pentachlorobiphenyl (PCB 95) amplifies ionotropic glutamate receptor signaling in embryonic cerebellar granule neurons by a mechanism involving ryanodine receptors. *Toxicol. Sci.* **77**, 72–82.

Grimm, F. A., Hu, D., Kania-Korwel, I., Lehmler, H. J., Ludewig, G., Hornbuckle, K. C., Duffel, M. W., Bergman, Å., *et al.* (2015). Metabolism and metabolites of polychlorinated biphenyls. *Crit. Rev. Toxicol.* **45**, 245–272.

Hwang, H. M., Green, P. G., and Young, T. M. (2006). Tidal salt marsh sediment in California, USA. Part 1: Occurrence and sources of organic contaminants. *Chemosphere* **64**, 1383–1392.

Hwang, S. A., Yang, B. Z., Fitzgerald, E. F., Bush, B., and Cook, K. (2001). Fingerprinting PCB patterns among Mohawk women. *J. Exposure Anal. Environ. Epidemiol.* **11**, 184–192.

Jacobson, J. L., and Jacobson, S. W. (1996). Intellectual impairment in children exposed to polychlorinated biphenyls in utero. *N. Engl. J. Med.* **335**, 783–789.

Kim, K. H., Bose, D. D., Ghogha, A., Riehl, J., Zhang, R., Barnhart, C. D., Lein, P. J., and Pessah, I. N. (2010). Para- and ortho-substitutions are key determinants of polybrominated diphenyl ether activity toward ryanodine receptors and neurotoxicity. *Environ. Health Perspect.* **119**, 519–526.

Kodavanti, P. R. S., and Curras-Collazo, M. C. (2010). Neuroendocrine actions of organohalogens: Thyroid hormones, arginine vasopressin, and neuroplasticity. *Front. Neuroendocrinol.* **31**, 479–496.

Kodavanti, P. R. S., and Tilson, H. A. (1997). Structure-activity relationships of potentially neurotoxic PCB congeners in the rat. *Neurotoxicology* **18**, 425–442.

Koh, W. X., Hornbuckle, K. C., and Thorne, P. S. (2015). Human serum from urban and rural adolescents and their mothers shows exposure to polychlorinated biphenyls not found in commercial mixtures. *Environ. Sci. Technol.* **49**, 8105–8112.

Kostyniak, P. J., Hansen, L. G., Widholm, J. J., Fitzpatrick, R. D., Olson, J. R., Helferich, J. L., Kim, K. H., Sable, H. J. K., *et al.* (2005). Formulation and characterization of an experimental PCB mixture designed to mimic human exposure from contaminated fish. *Toxicol. Sci.* **88**, 400–411.

Lacampagne, A., Fauconnier, J., and Richard, S. (2008). Ryanodine receptor and heart disease. *Méd. Sci.* **24**, 399–405.

Lehmler, H. J., Harrad, S. J., Hühnerfuss, H., Kania-Korwel, I., Lee, C. M., Lu, Z., and Wong, C. S. (2010). Chiral polychlorinated biphenyl transport, metabolism, and distribution: A review. *Environ. Sci. Technol.* **44**, 2757–2766.

Lilienthal, H., Korkalainen, M., Andersson, P. L., and Viluksela, M. (2015). Developmental exposure to purity-controlled polychlorinated biphenyl congeners (PCB74 and PCB95) in rats: Effects on brainstem auditory evoked potentials and catalepsy. *Toxicology* **327**, 22–31.

Lonky, E., Reihman, J., Darvill, T., Mather, J., and Daly, H. (1996). Neonatal behavioral assessment scale performance in humans influenced by maternal consumption of environmentally contaminated Lake Ontario fish. *J. Great Lakes Res.* **22**, 198–212.

Marek, R. F., Thorne, P. S., Wang, K., DeWall, J., and Hornbuckle, K. C. (2013). PCBs and OH-PCBs in serum from children and mothers in urban and rural US communities. *Environ. Sci. Technol.* **47**, 3353–3361.

Mariussen, E., and Fonnum, F. (2001). The effect of polychlorinated biphenyls on the high affinity uptake of the neurotransmitters, dopamine, serotonin, glutamate and GABA, into rat brain synaptosomes. *Toxicology* **159**, 11–21.

Mitchell, M. M., Woods, R., Chi, L. H., Schmidt, R. J., Pessah, I. N., Kostyniak, P. J., and LaSalle, J. M. (2012). Levels of select PCB and PBDE congeners in human postmortem brain reveal possible environmental involvement in 15q11-q13 duplication autism spectrum disorder. *Environ. Mol. Mutag.* **53**, 589–598.

Niknam, Y., Feng, W., Cherednichenko, G., Dong, Y., Joshi, S. N., Vyas, S. M., Lehmler, H. J., and Pessah, I. N. (2013). Structure-activity relationship of selected meta- and para-hydroxylated non-dioxin like polychlorinated biphenyls: From single RyR1 channels to muscle dysfunction. *Toxicol. Sci.* **136**, 500–513.

O'Neill, E. R., Sakowska, M. M., and Laver, D. R. (2003). Regulation of the calcium release channel from skeletal muscle by suramin and the disulfonated stilbene derivatives DIDS, DBDS, and DNDS. *Biophys. J.* **84**, 1674–1689.

Pessah, Cherednichenko, G., and Lein, P. J. (2010). Minding the calcium store: Ryanodine receptor activation as a convergent mechanism of PCB toxicity. *Pharmacol. Ther.* **125**, 260–285.

Pessah, I. N., Hansen, L. G., Albertson, T. E., Garner, C. E., Ta, T. A., Do, Z., Kim, K. H., and Wong, P. W. (2006). Structure−activity relationship for noncoplanar polychlorinated biphenyl congeners toward the ryanodine receptor-Ca^{2+} channel complex type 1 (RyR1). *Chem. Res. Toxicol.* **19**, 92–101.

Pessah, I. N., Lehmler, H. J., Robertson, L. W., Perez, C. F., Cabrales, E., Bose, D. D., and Feng, W. (2009). Enantiomeric specificity of (−)-2,2′,3,3′,6,6′-hexachlorobiphenyl toward ryanodine receptor types 1 and 2. *Chem. Res. Toxicol.* **22**, 201–207.

Pessah, I. N., Stambuk, R. A., and Casida, J. E. (1987). Ca^{2+}-activated ryanodine binding: Mechanisms of sensitivity and intensity modulation by Mg^{2+}, caffeine, and adenine nucleotides. *Mol. Pharmacol.* **31**, 232–238.

Pessah, I. N., Waterhouse, A. L., and Casida, J. E. (1985). The calcium-ryanodine receptor complex of skeletal and cardiac muscle. *Biochem. Biophys. Res. Commun.* **128**, 449–456.

Rayne, S., and Forest, K. (2010). Quantitative structure-activity relationship (QSAR) studies for predicting activation of the

ryanodine receptor type 1 channel complex (RyR1) by polychlorinated biphenyl (PCB) congeners. *J. Environ. Sci. Health A* **45**, 355–362.

Robinson, R., Carpenter, D., Shaw, M. A., Halsall, J., and Hopkins, P. (2006). Mutations in RYR1 in malignant hyperthermia and central core disease. *Hum. Mutat.* **27**, 977–989.

Samsó, M., Feng, W., Pessah, I. N., and Allen, P. (2009). Coordinated movement of cytoplasmic and transmembrane domains of RyR1 upon gating. *PLoS Biol.* **7**, e1000085.

Schantz, S., Seo, B., Wong, P., and Pessah, I. (1997). Long-term effects of developmental exposure to 2, 2', 3, 5', 6-pentachlorobiphenyl (PCB 95) on locomotor activity, spatial learning and memory and brain ryanodine binding. *Neurotoxicology* **18**, 457–467.

Schantz, S. L., Gasior, D. M., Polverejan, E., McCaffrey, R. J., Sweeney, A. M., Humphrey, H., and Gardiner, J. C. (2001). Impairments of memory and learning in older adults exposed to polychlorinated biphenyls via consumption of Great Lakes fish. *Environ. Health Perspect.* **109**, 605–611.

Shelton, J. F., Hertz-Picciotto, I., and Pessah, I. N. (2012). Tipping the balance of autism risk: Potential mechanisms linking pesticides and autism. *Environ. Health Perspect.* **120**, 944–951.

Simon, T., Britt, J. K., and James, R. C. (2007). Development of a neurotoxic equivalence scheme of relative potency for assessing the risk of PCB mixtures. *Regul. Toxicol. Pharmacol.* **48**, 148–170.

Stahl, L., Snyder, B., Olsen, A., and Pitt, J. (2009). Contaminants in fish tissue from US lakes and reservoirs: A National Probabilistic Study. *Environ. Monit. Assess.* **150**, 3–19.

Stamou, M., Streifel, K. M., Goines, P. E., and Lein, P. J. (2013). Neuronal connectivity as a convergent target of gene × environment interactions that confer risk for Autism Spectrum Disorders. *Neurotoxicol. Teratol.* **36**, 3–16.

Stenberg, M., Hamers, T., Machala, M., Fonnum, F., Stenius, U., Lauy, A. A., van Duursen, M. B., Westerink, R. H., *et al.* (2011). Multivariate toxicity profiles and QSAR modeling of non-dioxin-like PCBs—An investigation of in vitro screening data from ultra-pure congeners. *Chemosphere* **85**, 1423–1429.

Stewart, P. W., Lonky, E., Reihman, J., Pagano, J., Gump, B. B., and Darvill, T. (2008). The relationship between prenatal PCB exposure and intelligence (IQ) in 9-year-old children. *Environ. Health Perspect.* **116**, 1416–1422.

Stutzmann, G. E., Smith, I., Caccamo, A., Oddo, S., LaFerla, F. M., and Parker, I. (2006). Enhanced ryanodine receptor recruitment contributes to Ca^{2+} disruptions in young, adult, and aged Alzheimer's disease mice. *J. Neurosci.* **26**, 5180–5189.

Wayman, G. A., Bose, D. D., Yang, D., Lesiak, A., Bruun, D., Impey, S., Ledoux, V., Pessah, I. N., *et al.* (2012a). PCB-95 modulates the calcium-dependent signaling pathway responsible for activity-dependent dendritic growth. *Environ. Health Perspect.* **120**, 1003–1009.

Wayman, G. A., Yang, D., Bose, D. D., Lesiak, A., Ledoux, V., Bruun, D., Pessah, I. N., and Lein, P. J. (2012b). PCB-95 promotes dendritic growth via ryanodine receptor-dependent mechanisms. *Environ. Health Perspect.* **120**, 997–1002.

Westerink, R. H. (2014). Modulation of cell viability, oxidative stress, calcium homeostasis, and voltage-and ligand-gated ion channels as common mechanisms of action of (mixtures of) non-dioxin-like polychlorinated biphenyls and polybrominated diphenyl ethers. *Environ. Sci. Pollut. Res.* **21**, 6373–6383.

Wigestrand, M. B., Stenberg, M., Walaas, S. I., Fonnum, F., and Andersson, P. L. (2013). Non-dioxin-like PCBs inhibit [3H]WIN-35,428 binding to the dopamine transporter: A structure–activity relationship study. *Neurotoxicology* **39**, 18–24.

Wong, P. W., Brackney, W. R., and Pessah, I. N. (1997). Ortho-substituted polychlorinated biphenyls alter microsomal calcium transport by direct interaction with ryanodine receptors of mammalian brain. *J. Biol. Chem.* **272**, 15145–15153.

Wong, P. W., and Pessah, I. N. (1997). Noncoplanar PCB 95 alters microsomal calcium transport by an immunophilin FKBP12-dependent mechanism. *Mol. Pharmacol.* **51**, 693–702.

Yang, D., Kim, K. H., Phimister, A., Bachstetter, A. D., Ward, T. R., Stackman, R. W., Mervis, R. F., Wisniewski, A. B., *et al.* (2009). Developmental exposure to polychlorinated biphenyls interferes with experience-dependent dendritic plasticity and ryanodine receptor expression in weanling rats. *Environ. Health Perspect.* **117**, 426–435.

Zalk, R., Lehnart, S. E., and Marks, A. R. (2007). Modulation of the ryanodine receptor and intracellular calcium. *Annu. Rev. Biochem.* **76**, 367–385.